



UNIVERSITY OF LEEDS

This is a repository copy of *Quantum Confinement Effects in GeSn/SiGeSn Heterostructure Lasers*.

White Rose Research Online URL for this paper:
<http://eprints.whiterose.ac.uk/128331/>

Version: Accepted Version

Proceedings Paper:

Stange, D, Von den Driesch, N, Rainko, D et al. (10 more authors) (2018) Quantum Confinement Effects in GeSn/SiGeSn Heterostructure Lasers. In: Proceedings of IEDM 2017. 2017 IEEE International Electron Devices Meeting, 02-06 Dec 2017, San Francisco, CA, USA. IEEE , pp. 589-592. ISBN 978-1-5386-3559-9

<https://doi.org/10.1109/IEDM.2017.8268451>

U.S. Government work not protected by U.S. copyright. This is an author produced version of a paper published in the Proceedings of 2017 IEEE International Electron Devices Meeting (IEDM). Personal use of this material is permitted. Permission from IEEE must be obtained for all other uses, in any current or future media, including reprinting/republishing this material for advertising or promotional purposes, creating new collective works, for resale or redistribution to servers or lists, or reuse of any copyrighted component of this work in other works. Uploaded in accordance with the publisher's self-archiving policy.

Reuse

Unless indicated otherwise, fulltext items are protected by copyright with all rights reserved. The copyright exception in section 29 of the Copyright, Designs and Patents Act 1988 allows the making of a single copy solely for the purpose of non-commercial research or private study within the limits of fair dealing. The publisher or other rights-holder may allow further reproduction and re-use of this version - refer to the White Rose Research Online record for this item. Where records identify the publisher as the copyright holder, users can verify any specific terms of use on the publisher's website.

Takedown

If you consider content in White Rose Research Online to be in breach of UK law, please notify us by emailing eprints@whiterose.ac.uk including the URL of the record and the reason for the withdrawal request.



eprints@whiterose.ac.uk
<https://eprints.whiterose.ac.uk/>

Quantum Confinement Effects in GeSn/SiGeSn Heterostructure Lasers

D. Stange¹, N. von den Driesch¹, D. Rainko¹, T. Zabel², B. Marzban³, Z. Ikonic⁴, P. Zaumseil⁵, G. Capellini⁵, S. Mantl¹, J. Witzens³, H. Sigg², D. Grützmacher¹ and D. Buca¹

¹Peter Grünberg Institut 9, Forschungszentrum Jülich GmbH, Jülich, Germany, E-mail: d.m.buca@fz-juelich.de

²Laboratory for Micro- and Nanotechnology (LMN), Paul Scherrer Institute, CH-5232 Villigen, Switzerland

³Institute of Integrated Photonics, RWTH Aachen, 52074 Aachen, Germany

³Institute of Microwaves and Photonics, School of Electronic and Electrical Engineering, University of Leeds, Leeds LS2 9JT, UK

⁴IHP, Im Technologiepark 25, 15236 Frankfurt (Oder), Germany

Abstract— The development of a light source on Si, which can be integrated in photonic circuits together with CMOS electronics, is an outstanding goal in the field of Silicon photonics. This could e.g. help to overcome bandwidth limitations and losses of copper interconnects as the number of high-speed transistors on a chip increases. Here, we discuss direct bandgap group IV materials, GeSn/SiGeSn heterostructures and resulting quantum confinement effects for laser implementation. After material characterization, optical properties, including lasing, are probed via photoluminescence spectrometry. The quantum confinement effect in GeSn wells of different thicknesses is investigated. Theoretical calculations show strong quantum confinement to be undesirable past a certain level, as the very different effective masses of Γ and L electrons lead to a decrease of the L- to Γ -valley energy difference. A main limiting factor for lasing devices turns out to be the defective region at the interface to the Ge substrate due to the high lattice mismatch to GeSn. The use of buffer technology and subsequent pseudomorphic growth of multi-quantum-wells structures offers confinement of carriers in the active material, far from the misfit dislocations region. Performance is strongly boosted, as a reduction of lasing thresholds from 300 kW/cm² for bulk devices to below 45 kW/cm² in multi-quantum-well lasers is observed at low temperatures, with the reduction in threshold far outpacing the reduction in active gain material volume.

I. INTRODUCTION

Many approaches to develop an infrared laser source on Silicon are under investigation, in order to push the integration of Silicon photonics with CMOS technology. Integration of electro-optical components promises the decrease of power consumption and heat production as well as a rise of communication bandwidth [1], [2]. One material system option for such semiconductor lasers are direct bandgap GeSn alloys, which can be epitaxially grown on standard Si wafers. Alloying Ge with Sn changes the electronic band structure and pulls down the conduction band at Γ faster than that at L. This can lead to the transition from a fundamentally indirect to direct bandgap semiconductor behavior. The existence of a direct bandgap and optically pumped lasing has already been shown for bulk GeSn alloys with various Sn concentrations, which allows tunable emission at wavelengths between 2 μ m and

3.1 μ m [3]–[6]. A lot of potential to improve performance remains, since the maximum lasing temperature is still limited to 180 K [6], lasing thresholds are well above 100 kW/cm² for optical pumping, and electrically driven laser sources are completely missing. This contribution will concentrate on reduction of the threshold by employing heterostructures, including quantum-well designs. The effects of local carrier confinement and of quantum confinement are shown via photoluminescence studies, and lasing from microdisk cavities is presented.

II. STRUCTURAL PROPERTIES AND QUANTUM CONFINEMENT

All presented heterostructures are grown via chemical vapor deposition in an AIXTRON Tricent reactor. Disilane, digermane and tin tetrachloride are used as precursor gases. The material is grown on Ge buffered 200 mm silicon wafers. To reduce the compressive strain in the structures, an additional Ge_{0.9}Sn_{0.1} buffer layer of 200 nm thickness is used for strain relaxation before starting heterostructure growth. One further advantage of the GeSn buffer technology is the possibility to constrain misfit dislocations at the interface between the Ge virtual substrate and the GeSn buffer, away from the active device region. Three different structures are presented here: one double heterostructure (DHS) and two multi-quantum-well structures with well/barrier thicknesses of (22/22) nm (MQW1) and (12/16) nm (MQW2), respectively. The well material Ge_{0.87}Sn_{0.13} is embedded in Si_{0.05}Ge_{0.82}Sn_{0.13} barriers. Fig. 1a and b show secondary ion mass spectrometry (SIMS) measurements of MQW1 and MQW2. Incorporation of Sn and Si in wells and barriers is homogeneous across the layers. An X-ray diffraction (XRD) reciprocal space map (RSM) of MQW1 in Fig. 2 confirms pseudomorphic growth on top of the GeSn buffer. In contrast, misfit dislocations at the interface between the lower SiGeSn cladding and the active GeSn region of the DHS are revealed by the transmission electron microscopy (TEM) micrograph in Fig. 3. This indicates that the active GeSn layer relaxes even further on top of the GeSn buffer, resulting in additional non-radiative recombination paths.

Theoretical calculations, based on an 8-band k-p method and including the influence of strain via deformation potentials, are used to obtain information on band structure properties such

as bandgap, energy offset between L and Γ ($\Delta E_{L-\Gamma}$) and the formation of quantized states. One distinct uncertainty regarding these calculations is the value of the optical SiSn bowing parameter b_{SiSn} , whose reported values are spread between 3.9 and 24 eV in the literature. Calculations presented here correspond to $b_{\text{SiSn}} = 3.9$ eV. Bandgaps and $\Delta E_{L-\Gamma}$ are calculated for all three structures and are given in Table 1. Additionally, effects of quantization, dependent on the well thickness, are shown in Fig. 4. With decreasing well thickness the quantized Γ electron states are lifted much faster than quantized L states (due to very different effective masses) and a direct bandgap semiconductor will turn into an indirect one at a certain point. Therefore, very thin wells in a GeSn/SiGeSn system may not be the best choice for the design of an efficient laser. To verify calculated bandgaps, photoluminescence measurements, performed in step scan mode with an excitation wavelength of 532 nm, are demonstrated in Fig. 5. Taking into account (slight) differences in Sn concentration and strain of the different structures, the PL peak positions fit quite well to the calculated values. For MQW2 the effect of quantization is visible in terms of a distinct blue shift compared to MQW1. The temperature dependent PL intensity, Fig. 6, shows the clear favorite for laser performance. The increase of intensity with decreasing temperature is one order of magnitude higher for MQW1 than for DHS. Since similar barrier heights should be present in both structures, the effect can be attributed to a higher non-radiative recombination rate in case of DHS, due to the presence of misfit dislocations at the interface. However, this effect is only visible below 150 K. Above it, carriers in MQW1 can escape from the well region due to their increased thermal energy and are able to non-radiatively recombine at the defective bottom interface. Nevertheless, PL analysis shows the great potential of GeSn/SiGeSn multi wells as future gain material.

III. LASING IN HETEROSTRUCTURES

Microdisk cavities of 8 μm diameter were fabricated with an undercut of ~ 3.5 μm from DHS and MQW1 according to the process flow described in reference [4]. A scanning electron micrograph (SEM) of DHS is shown in Fig. 7. Microdisk cavities are pumped by either a Nd:YAG or a 1550 nm laser from the top, and the scattered laser light is collected in the same direction. Light-in light-out (LL) curves of DHS, pumped by the Nd:YAG laser, show a strongly increased light emission once the lasing threshold is reached, Fig. 8. Furthermore, the typical linewidth narrowing is observed, when lasing sets in. The same kind of behavior is also found for MQW1, as shown in Fig. 9. The full width at half maximum (FWHM) here appears larger than in DHS, which is related only to the used spectrometer resolution. Lasing thresholds at different temperatures are evaluated as the intersection of a linear fitted curve. The linear fit is applied on the one hand to the LL values in lasing onset region (recorded with lock-in technique), and on the other hand to the integrated individual spectra. Mean values of both approaches with their standard deviation are depicted for different excitations and structures in Fig. 10. In comparison to previously measured threshold values for bulk GeSn layers [4], DHS microdisks do not show any distinct advantage. As

previously discussed, lasing performance in both types of samples is strongly limited by the presence of defects adjacent to the active region. However, a clear difference is visible in case of MQW1, where the lasing threshold is reduced to around 45 kW/cm² at 20 K (1550 nm). Confining the carriers in many wells, keeping them away from any misfit dislocations by conformal growth on top of a buffer layer region seems to be advantageous for optimized laser structures.

Comparing high resolution spectra of 4 cm⁻¹ in Fig. 11, only a very slight energy shift of 0.48 meV can be observed, implying that the effect of heating is very slight. Comparing the highest reachable lasing temperature in each structure, microdisk lasers seem to work at ~ 20 K higher temperatures if pumped by a 1550 nm laser (Fig. 10). At temperatures above 120 K, carrier confinement in GeSn wells is weak (offset GeSn-SiGeSn ~ 30 -50 meV) and carriers can escape from the active region. The MQW characteristics then look similar to those of the DHS (compare emissions in Fig. 6). Additionally, increased Auger recombination and free carrier absorption occur at higher temperatures. This is exacerbated by carrier excitation at higher energies, influencing the maximum lasing temperature.

IV. CONCLUSION

In conclusion, the epitaxy and confinement effects in GeSn/SiGeSn MQW and double heterostructures was presented. Optically pumped lasing from group IV (Si)GeSn heterostructures was demonstrated for the first time in microdisk cavities. The effects of both carrier and quantum confinement were discussed and found to offer the possibility of reducing the lasing threshold by an order of magnitude. For improved lasing devices the ternary SiGeSn cladding layers play a major role and the epitaxy should be pushed towards high Si contents ternaries which offer a stronger carrier confinement especially important for reaching room temperature lasing.

ACKNOWLEDGMENT

The authors acknowledge the Deutsche Forschungsgemeinschaft (DFG) for funding of the project “(Si)GeSn laser for Silicon Photonics”.

REFERENCES

- [1] R. Soref, “Group IV photonics: Enabling 2 μm communications,” *Nat. Photonics*, vol. 9, no. 6, pp. 358–359, May 2015.
- [2] D. J. Richardson, “Silicon photonics: Beating the electronics bottleneck,” *Nat. Photonics*, vol. 3, no. 10, pp. 562–564, Oct. 2009.
- [3] S. Wirths, R. Geiger, et al., “*Nat. Photonics*, vol. 9, no. January, pp. 88–92, Jan. 2015.
- [4] D. Stange, S. Wirths, R. Geiger et al., “Optically Pumped GeSn Microdisk Lasers on Si,” *ACS Photonics*, vol. 3, no. 7, pp. 1279–1285, Jul. 2016.
- [5] S. Al-kabi et al., “An optically pumped 2.5 μm GeSn laser on Si operating at 110 K,” *Appl. Phys. Lett.*, vol. 109, p. 171105, 2016.
- [6] V. Reboud et al., “Optically pumped GeSn micro-disks with 16 % Sn lasing at 3 . 1 μm up to 180K,” pp. 1–15.

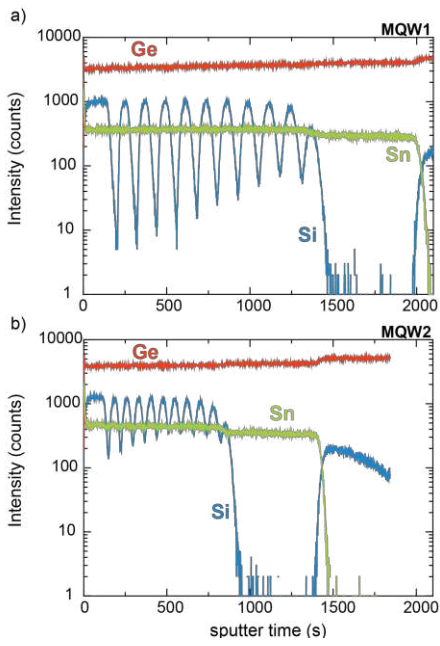


Fig. 1. Secondary ion mass spectrometry line scans of multi quantum well structures with well/barrier thicknesses of (22/22) nm and (12/16) nm in a) and b), respectively.

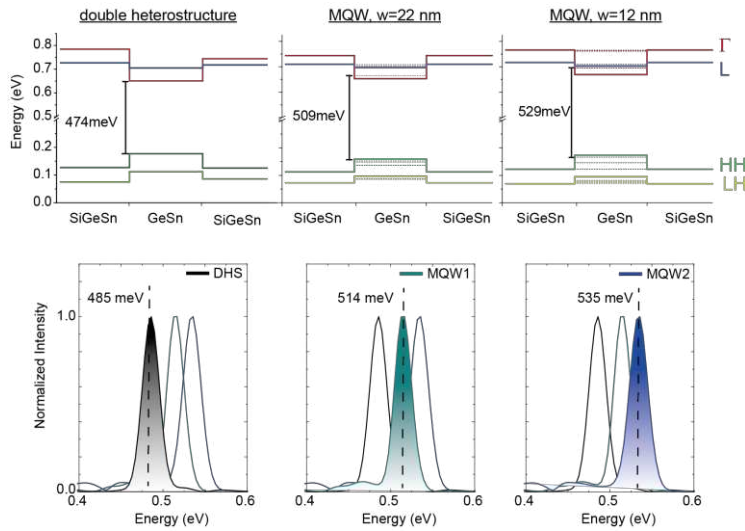


Fig. 5. Band structure calculations and low temperature PL (4 K) for all three structures showing a reasonable agreement.

	DHS	MQW1	MQW2
E_g (meV)	474	509	529
$\Delta E_{\Gamma-L}$ (eV)	83	32	8

Table 1. Bandgap and $\Delta E_{\Gamma-L}$ calculated for three structures. In case of quantized states, always the lowest energy level is regarded.

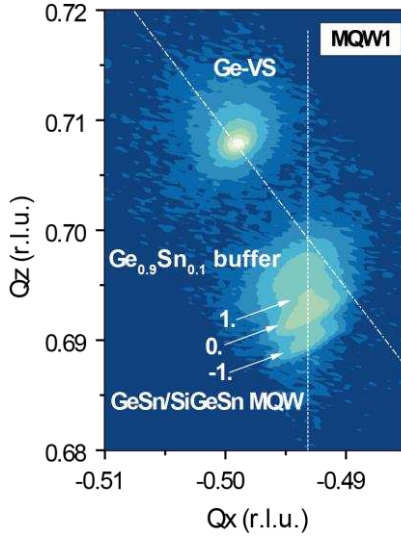


Fig. 2. X-Ray Diffraction reciprocal space map of MQW1 showing conformal growth of multi-wells on top of a GeSn buffer without further relaxation.

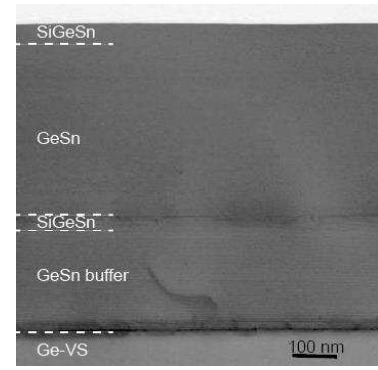


Fig. 3. TEM micrograph of DHS showing misfit dislocations at the interface between the lower SiGeSn cladding layer and the active GeSn region.

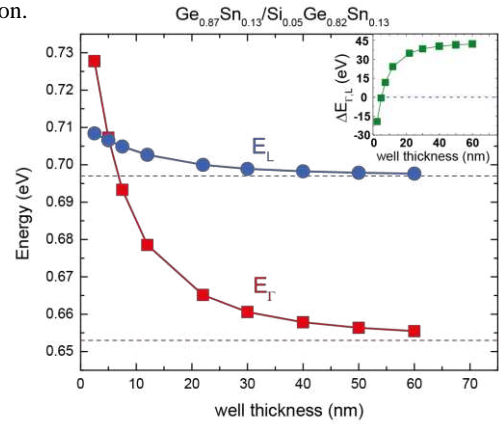


Fig. 4. Band structure calculations of MQW structures for different well thicknesses. ΔE_{L-L} becomes smaller in thinner wells due to the smaller effective mass of Γ electrons, eventually turning the direct GeSn alloy into an indirect one below 7 nm.

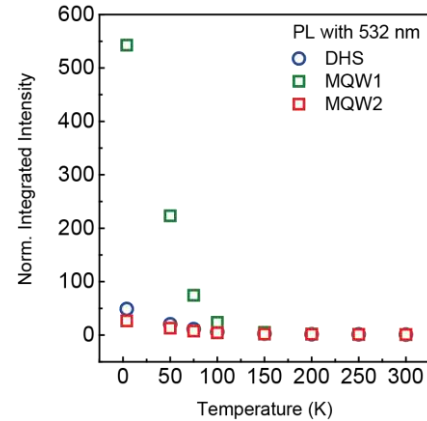


Fig. 6. Integrated PL Intensity, excited with a 532 nm laser, is shown dependent on temperature. Below 100 K a huge intensity increase can be observed for MQW1.

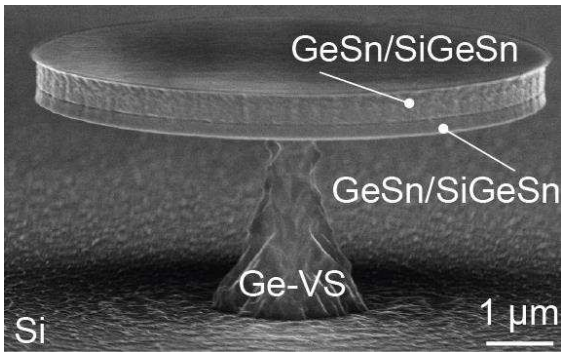


Fig. 7. Scanning electron micrograph of a microdisk cavity of 8 μm diameter, which was processed by standard Si technology from DHS.

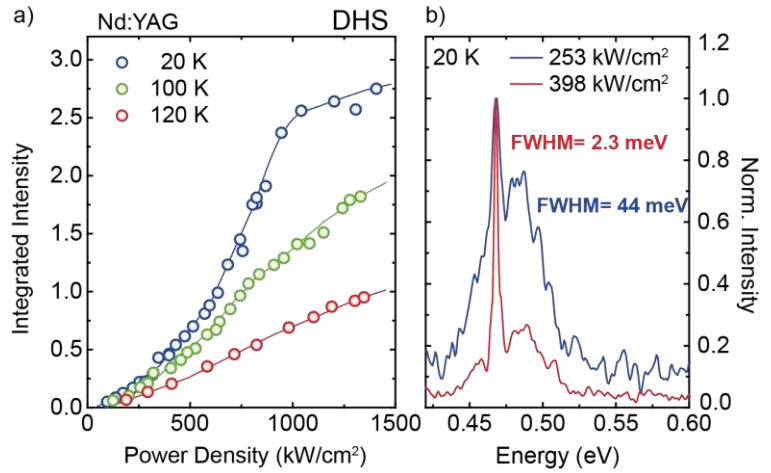


Fig. 8. Lasing characteristics of a DHS microdisk cavity. Light-in light-out curves at different temperatures (a) and linewidth collapse at 20 K visible above the lasing threshold (b).

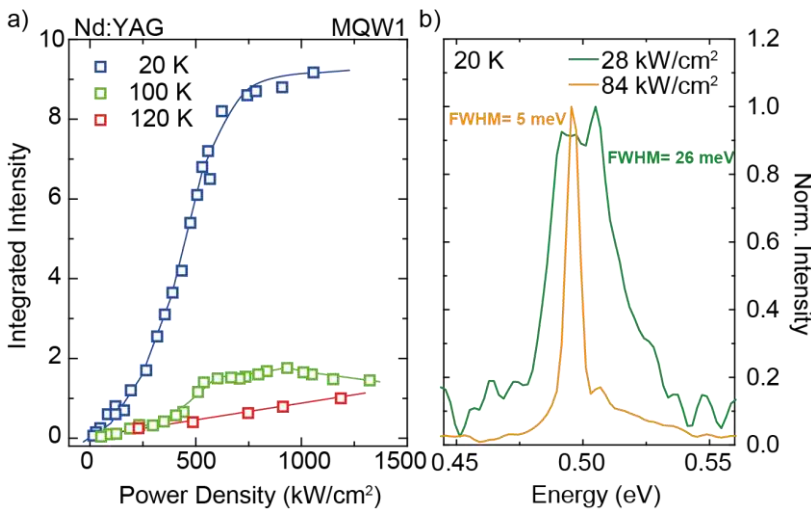


Fig. 9. Lasing characteristics of a microdisk cavity from MQW1. Light-in light-out curves at different temperatures (a) and linewidth collapse at 20 K are visible for certain excitation densities (b).

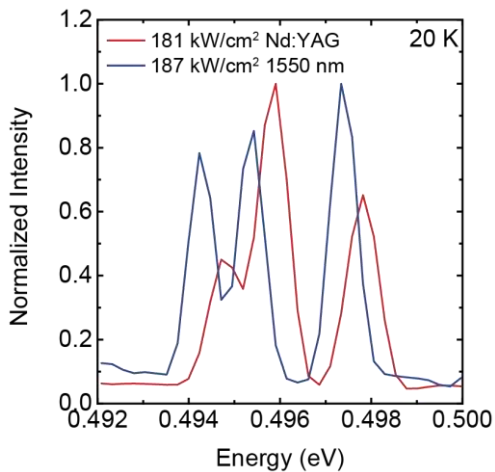


Fig. 11. High resolution spectra for MQW1 microdisk laser pumped by different excitation lasers.

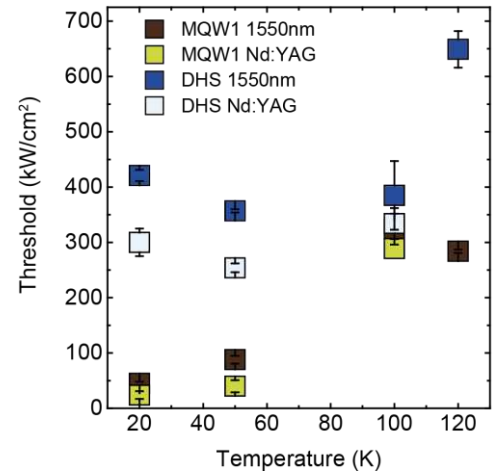


Fig. 10. Overview of different lasing thresholds, taking into account fits of light-in light-out curves as well as fits of integrated spectra. Values are given for MQW1 and DHS at different temperatures and both pumping lasers.